

Extruded single-mode high-index-core one-dimensional microstructured optical fiber with high index-contrast for highly nonlinear optical devices

Xian Feng, Tanya M. Monro, Periklis Petropoulos, Vittoria Finazzi, and David J.

Richardson

Optoelectronics Research Centre, University of Southampton, Southampton, SO17 1BJ,

United Kingdom

We report the first fabrication of a high-index-core one-dimensional microstructured optical fiber with high index-contrast layers. The extrusion technique is utilized to fabricate a microstructured preform with a number of concentric high-index-contrast layers. Single mode guidance and the high effective nonlinearity of $260 \pm 30 \text{W}^{-1} \text{km}^{-1}$ were observed in the fiber at $1.55 \mu\text{m}$, indicating its promise in the applications of highly nonlinear optical devices.

Microstructured optical fibers (MOFs), which are also known as photonic crystal fibers (PCFs)¹ or holey fibers (HFs), are attractive for broad range of applications due to the unique optical performance that can be achieved. Novel optical properties such as photonic bandgaps, single-mode operation combined with very large mode area, dispersion management and high nonlinearity can be achieved in this new type of optical fiber². Light can be guided either in a low-index core due to bandgap-guiding, or in a high-index core due to the more conventional index-guiding mechanism. Compared to silica glass based MOFs, non-silica glass based MOFs show great promise as a result of the high refractive index, the high nonlinear refractive index, low processing temperature and high transparency in mid-IR region (2-5 μm)³ that can be achieved in non-silica glasses.

Previous works on MOFs^{1,4} reveal that the main factors responsible for their unique optical performance are the (1) wavelength-scale features within the microstructured cladding and (2) high index-contrast between the dielectric materials that constitute the fiber cladding. This is true regardless of the guiding mechanism of the fiber, or whether the microstructured cladding is 1-dimensional (1D)^{4,5} or 2-dimensional (2D)¹ in nature. Fig.1 illustrates the typical microstructures of 1D and 2D MOFs.

Due to the high purity and excellent homogeneity of pure silica glass, single pure silica glass based MOFs have shown their potential to achieve extremely low attenuation than the conventional silica fiber⁶. However, the use of a single material is not necessary in order to achieve the novel and useful optical properties of MOFs. In fact, the existence of air within the holes results in the unavoidable deformation of the microstructure in the cladding region during fiber manufacture, which consequently makes it challenging to

fabricate fibers with pre-determined optical performance characteristics. Following this approach, we previously reported the fabrication of the first all-solid 2D all-solid MOF, also called a SOHO fiber (SOLid HOley fiber), based on two types of silicate glasses with a high-index-contrast of 0.23 at $1.55\mu\text{m}$ ⁷. The SOHO fiber has a microstructured cladding of the typical holey fiber and all the holes are filled with low-index glass. This approach enabled fibers to be drawn to any practical dimensions without any observable deformations of the transverse cladding structure⁷. High nonlinearity and near-zero dispersion have been achieved in SOHO fibers⁷.

Moreover, the concept of an all-solid microstructured optical fiber even permits us to fabricate 1D microstructured cladding in addition to the more usual 2D triangular microstructure (see Fig.1). Prediction indicates that high-index-core 1D MOFs can have useful optical characteristics such as ultra-flat dispersion⁸, which can be difficult to be achieved in 2D high-index-core MOFs without significantly compromising the nonlinearity that can be achieved.

In this work we report what we believe to be the first successful fabrication of a high-index-core 1D MOF based on high index-contrast optical glasses. The microstructured preform with multiple coaxial rings was fabricated using the extrusion technique⁹. In the earliest works on extrusion of glass¹⁰, it was established that when glass is extruded through a channel with circular cross-section, the flow behavior obeys the Hagen-Poiseuille law, i.e., the isothermal laminar volumetric flow rate V is given by $V = \pi\Delta p \cdot r^4 / (8\eta \cdot l)$, where Δp is the pressure difference between the entrance and exit of the channel, η the glass viscosity, and r and l its radius and length, respectively. Due to the friction at the die wall, an inhomogeneous distribution of flow velocity V is formed

across the die aperture. Given a completely stagnant layer adjacent to the wall, the velocity profile becomes parabolic: $V = \Delta p \cdot (r^2 - x^2) / (4\eta \cdot l)$, where x is the radial coordinate, and $x=r$ at the interference between the flow and the channel. Hence a macroscopically structured preform with multiple coaxial rings can be fabricated by extruding alternatively stacked high- and low-index glass discs. This is shown schematically in Fig. 2b. Note that very recently a similar approach using disc-stacking extrusion was used to fabricate 1D microstructured glass-polymer preforms with both solid- and hollow-cores¹¹. However, the fabrication of fiber from these preforms was not reported to the best of our knowledge.

As in Ref. [7], a lead-oxide (PbO) containing borosilicate glass (PbO>30mol.%) with refractive index of $n=1.76$ at 1550nm (referred as B1 thereafter), and a potassium-fluoride (KF) containing borosilicate glass with index $n=1.53$ at 1550nm (referred as H1 thereafter) were selected as the materials for this high-index-core 1D MOF. Fig.2(a) shows the viscosity curves of these two glasses measured on a Perkin Elmer TMA-7 Thermomechanical Analyzer using the parallel-disc technique¹². Fig.2a shows that these two types of glasses are thermally matched for both extrusion and fiber-drawing.

As shown in Fig.2(b), 1.0 mm thick high-index glass discs were stacked alternately with 2.0 mm thick low-index glass discs. The stack of glass discs was heated to above the glass softening temperature (corresponding viscosity: $\sim 10^9$ - 10^7 poise). Using an applied force of up to 1 ton, the viscoelastic glass flow was pressed through the circular exit, and a preform with the structure of multiple ring layers was formed. The extruded preform was then reduced in scale on a fiber-drawing tower into cane with $790 \pm 10 \mu\text{m}$ outer-diameter (OD). A piece of 80mm-long uniform cane was selected and inserted within a

high-index B1 glass jacket-tube with 18mm OD and $800 \pm 10 \mu\text{m}$ inner-diameter (ID). Finally, this rod-in-tube assembly was pulled into the high-index-core 1D MOF. The total fiber yield was near 400 meters, and fibers with OD ranging from 115 to $825 \mu\text{m}$ were produced.

Figs.3a and b show Scanning Electronic Microscope (SEM) photographs of this high-index-core 1D MOF with $825\mu\text{m}$ and $135\mu\text{m}$ OD, respectively. The high-index region (with density $\rho = 5.2 \text{ g/cm}^3$) shows higher brightness than the low-index region (with density $\rho = 2.9 \text{ g/cm}^3$), due to the intensity contrast of the backscattered electrons from the sample with different matter density⁷. The high-index-core is surrounded by 9 alternate rings of coaxial low-index and high-index layers. Observe that the resulting core and rings are highly circular and concentric. After normalizing parameters of the microstructure such as the core diameter and the thickness of each individual ring by the OD of the fiber, it is observed that for all the fibers with the outer diameter ranging from $825\mu\text{m}$ to $135\mu\text{m}$, the microstructure of this high-index-core 1D MOF is dimension-independent, consistent with previous observations in the 2D-structured SOHO fiber⁷. This is believed to be one of the most important advantages of an all-solid MOF relative to an air-filled holey fiber, since it allows the stable and repeatable definition of transverse structure that is essential for achieving optical fibers with pre-determined optical characteristics.

The velocity of the glass flow within the extrusion die is determined by (1) the friction coefficient between the glass flow and the metal die and (2) the internal friction of the glass within the channel in the die¹⁰. Additionally, when different glasses are employed during extrusion, the effect of the internal friction of the glass flow becomes

more complicated due to the thermal mismatch between the two glasses. As a result, although the starting high-index (or low-index) glass discs were uniform in thickness, significant thickness variations are evident in the final ring fiber (see Fig.3). By adjusting the thickness of the starting discs to compensate this non-uniformity, it should be possible to achieve preforms with controllably thick ring layers such as periodically spaced ring layers if required.

Fiber with a $1.9\mu\text{m}$ core diameter (corresponding to a fiber OD of $175\mu\text{m}$) was selected for optical characterization. Fig. 4(a) shows the index profile of this fiber deduced from the SEM photo, assuming the refractive indices of all regions are unchanged after fiber-drawing. It is seen that the thickness of the high-index rings ranges between 100 nm and 250 nm, while the thickness of the low-index rings ranges between 120 nm and 780 nm.

The guidance properties of this $1.9\mu\text{m}$ core fiber were evaluated using a range of laser sources including a CW Argon ion laser operating at 514 nm, a laser diode at 635 nm, a Nd:YLF laser at 1047nm and a erbium doped fiber laser operating at 1560nm. A COHU 7512 CCD camera was used with Spiricon LBA-PC v 3.23 software (Spiricon Inc., Logan, UT, USA) for imaging the near-field beam profile from the output end of the fiber.

Fig.4(b) shows the guidance at 514 nm, 635 nm, 1047 nm and 1560 nm. It is seen that at the short wavelength of 514 nm, the fiber is at least two moded, and light can even be weakly guided in the thickest high-index layer, while at 635 nm, light is guided within the core alone, and the fiber is still slightly multimode. At the relatively longer

wavelengths of 1047 nm and 1560 nm, only the Gaussian fundamental mode can be observed in the high-index core.

Using the cutback technique, the fiber loss was measured as 3.6 ± 0.5 dB/m at 1560 nm. Our modeling indicates that the confinement loss of this 1D MOF at 1560 nm is ≤ 1 dB/m. Note that this disc-stacking extrusion technique can be extended to introduce more layers into the cladding, which would improve the confinement of this fiber.

The effective nonlinearity of this 1D MOF with $1.9\mu\text{m}$ core diameter was measured by using the self-phase-modulation (SPM) based technique firstly used by Boskovic et al¹³. Using a CW high power dual-frequency beat signal at 1560nm as the pump signal, the optical spectrum at the end of the fiber exhibits peaks at multiples of this beat frequency because of the SPM-induced phase modulation (see Fig.5). Neglecting the fiber dispersion due to the short-length of the measured fiber, the nonlinear phase shift experienced by the beat signal propagating along the fiber can be expressed as $\varphi_{SPM} = (2\pi / \lambda) \cdot (n_2 / A_{eff}) \cdot L_{eff} \cdot P$, where λ is the wavelength of the signal, P the average power of the signal, L_{eff} the effective length of the fiber ($L_{eff} = [1 - \exp(-\alpha \cdot L)] / \alpha$, α : the fiber loss, and L : the total fiber length), n_2 the nonlinear refractive index of the core material, and A_{eff} the effective mode area. The ratio of the peak heights depends only on the nonlinear phase shift φ_{SPM} . By varying the signal power, the effective nonlinearity of the fiber, $\gamma (= (2\pi / \lambda) \cdot (n_2 / A_{eff}))$ can be deduced from the ratio of the intensities of the first sideband to the spectral intensity at the fundamental frequencies by the linear least-square-fitting¹³. The effective nonlinearity γ of this 1D MOF with $1.9 \mu\text{m}$ core diameter is measured as $260 \pm 30 \text{ W}^{-1}\text{km}^{-1}$, which is 260 times higher than standard single mode

silica fiber, indicating that it is a promising candidate for the applications of highly nonlinear optical devices.

In summary, we have demonstrated the first successful fabrication of high-index-core 1D MOF with high index-contrast layers. Robust single-mode guidance has been observed at both 1047 and 1560 nm. The propagation loss of 3.6 dB/m has been measured at the wavelength of 1560nm. A high effective nonlinearity of $260 \text{ W}^{-1}\text{km}^{-1}$ has been measured at 1560 nm in this fiber, highlighting the potential application of this new fiber in highly nonlinear optical devices. In addition, we have demonstrated a preform fabrication technique that has the flexibility to produce all-glass 1D structured fibers either with periodically structured layers or with controllable variations in layer thicknesses.

FIGURE 1, Xian Feng et al, submitted to Applied Physics Letters

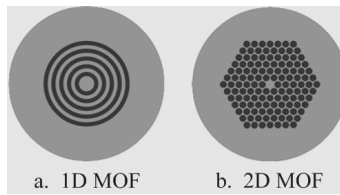


FIGURE 2, Xian Feng et al, submitted to Applied Physics Letters

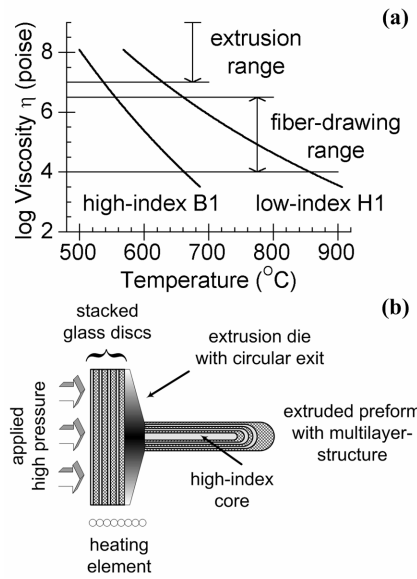


FIGURE 3, Xian Feng et al, submitted to Applied Physics Letters

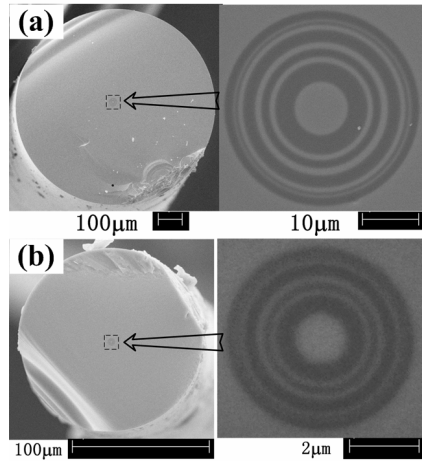


FIGURE 4, Xian Feng et al, submitted to Applied Physics Letters

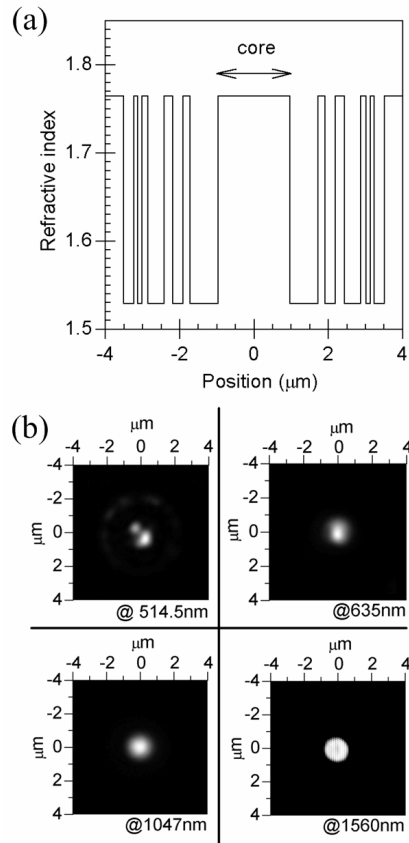


FIGURE 5, Xian Feng et al, submitted to Applied Physics Letters

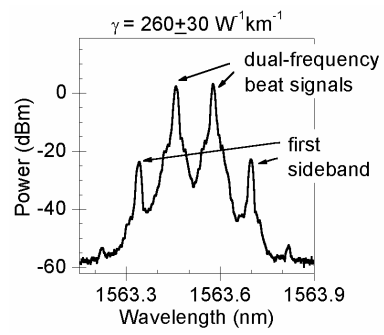


Figure captions

Fig. 1 Illustration of 1D and 2D MOFs.

Fig. 2 (a) Schematic of disc-stacking extrusion to manufacture the preform with multi-ring structured cladding. (b) Measured viscosity curves of high-index glass (B1) and low-index glass (H1).

Fig. 3 SEM photographs of high-index-core 1D MOF with various ODs. (a) Whole view and zoomed center of the fiber with 825 μm OD; (b) whole view and zoomed center of the fiber with 135 μm OD.

Fig. 4 (a) Refractive index profile along the center of the fiber with 1.9 μm core diameter. (b) Guidance at 514.5nm, 635nm, 1047nm and 1560nm.

Fig. 5 One of the measured spectrums for the nonlinear mixing in this solid-core 1D fiber (input power: 420mW, fiber length: 67cm). Note the large increase in power in the sidebands due to self-phase modulation.

-
- ¹ J. C. Knight, T. A. Birks, P. St. J. Russell, and D. M. Atkin, *Opt. Lett.* **21**, 1547 (1996).
- ² P. Russell, *Science* **299**, 358 (2003).
- ³ T. M. Monro, Y. D. West, D. W. Hewak, N. G. R. Broderick, and D. J. Richardson, *Electron. Lett.* **36**, 1998 (2000).
- ⁴ B. Temelkuran, S. D. Hart, G. Benoit, J. D. Joannopoulos, and Y. Fink, *Nature (London)* **420**, 650 (2002).
- ⁵ P. Yeh, A. Yariv, and E. Marom, *J. Opt. Soc. Am. B* **68**, 1196 (1978).
- ⁶ K. Tajima, J. Zhou, K. Nakajima, and K. Sato, *J. Lightwave Tech.* **22**, 7 (2004).
- ⁷ X. Feng, T. M. Monro, P. Petropoulos, V. Finazzi, and D. W. Hewak, *Opt. Express* **11**, 2225 (2003).
- ⁸ J. A. Monsoriu, E. Silvestre, A. Ferrando, P. Andres, and J. J. Miret, *Opt. Express* **11**, 1400 (2003).
- ⁹ E. Roeder, *J. Non-Cryst. Solids* **5**, 377 (1971).
- ¹⁰ E. Roeder, *J. Non-Cryst. Solids* **7**, 203 (1972).
- ¹¹ D. J. Gibson and J. A. Harrington, *J. Appl. Phys.* **95**, 3895 (2004).
- ¹² E. H. Fontana, *Amer. Ceram. Soc. Bull.* **49**, 594 (1970).
- ¹³ A. Boskovic, S. V. Chernikov, J. R. Taylor, L. Gruner-Nielsen, and O. A. Levring, *Opt. Lett.* **21**, 1966 (1996).